A synthetic biology-based device prevents liver injury in mice

Author(s):
Bai, Peng; Ye, Haifeng; Xie, Mingqi; Saxena, Pratik; Zulewski, Henryk; Charpin-El Hamri, Ghislaine; Djonov, Valentin; Fussenegger, Martin (ID)

Permanent link:
https://doi.org/10.3929/ethz-b-000116099

CrossMark

EASL **JOURNAL OF HEPATOLOGY**

A synthetic biology-based device prevents liver injury in mice

Peng Bai[1], Haifeng Ye[1,2], Mingqi Xie[1], Pratik Saxena[1], Henryk Zulewski[1,3,4],
Ghislaine Charpin-El Hamri[5], Valentin Djonov[6], Martin Fussenegger[1,7,*]

[1]Department of Biosystems Science and Engineering, ETH Zurich, Mattenstrasse 26, CH-4058 Basel, Switzerland; [2]Shanghai Key Laboratory of Regulatory Biology, Institute of Biomedical Sciences and School of Life Sciences, East China Normal University, Dongchuan Road 500, Shanghai 200241, China; [3]Faculty of Medicine, University of Basel, Petersgraben 4, CH-4031 Basel, Switzerland; [4]Division of Endocrinology and Diabetes, Stadtspital Triemli, Birmensdorferstrasse 497, CH-8063 Zurich, Switzerland; [5]Département Génie Biologique, Université Claude Bernard 1, 43 Boulevard du 11 Novembre 1918, F-69100 Villeurbanne, France; [6]Institute of Anatomy, University of Berne, Baltzerstrasse 2, CH-3000 Berne, Switzerland; [7]Faculty of Science, University of Basel, Mattenstrasse 26, CH-4058 Basel, Switzerland

Background & Aims: The liver performs a panoply of complex activities coordinating metabolic, immunologic and detoxification processes. Despite the liver's robustness and unique self-regeneration capacity, viral infection, autoimmune disorders, fatty liver disease, alcohol abuse and drug-induced hepatotoxicity contribute to the increasing prevalence of liver failure. Liver injuries impair the clearance of bile acids from the hepatic portal vein which leads to their spill over into the peripheral circulation where they activate the G-protein-coupled bile acid receptor TGR5 to initiate a variety of hepatoprotective processes.
Methods: By functionally linking activation of ectopically expressed TGR5 to an artificial promoter controlling transcription of the hepatocyte growth factor (HGF), we created a closed-loop synthetic signalling network that coordinated liver injury-associated serum bile acid levels to expression of HGF in a self-sufficient, reversible and dose-dependent manner.
Results: After implantation of genetically engineered human cells inside auto-vascularizing, immunoprotective and clinically validated alginate-poly-(L-lysine)-alginate beads into mice, the liver-protection device detected pathologic serum bile acid levels and produced therapeutic HGF levels that protected the animals from acute drug-induced liver failure.
Conclusions: Genetically engineered cells containing theranostic gene circuits that dynamically interface with host metabolism may provide novel opportunities for preventive, acute and chronic healthcare.

Lay summary: Liver diseases leading to organ failure may go unnoticed as they do not trigger any symptoms or significant discomfort. We have designed a synthetic gene circuit that senses excessive bile acid levels associated with liver injuries and automatically produces a therapeutic protein in response. When integrated into mammalian cells and implanted into mice, the circuit detects the onset of liver injuries and coordinates the production of a protein pharmaceutical which prevents liver damage.

Introduction

The liver is associated with over 500 functions which include the clearance of the blood from toxic compounds, drugs and infectious agents, the control of blood fat and glucose levels, and the recovery, processing and conversion of digested food into metabolic energy [1]. The processing of digested food requires the production of bile and its major component, the bile acids. Bile acids are synthesized from cholesterol in the liver, secreted by the hepatocytes into bile canaliculi and stored in the gall bladder [2]. After each meal, bile acids are released into the duodenum to emulsify ingested fats and other lipophilic nutrients, reabsorbed in the terminal ileum and transported back to the liver via the portal vein, a process known as enterohepatic circulation [2,3]. Efficient clearance and recycling of bile acids from the portal vein ensures low bile acid levels in the peripheral circulation, which increase only marginally after each meal [2]. However, in patients suffering from diverse liver diseases such as cirrhosis, cholestasis, hepatitis and liver cancer, fasting blood bile acid levels are markedly increased due to the impaired hepatic clearance of bile acids from the portal vein [4–10]. Serum bile acid (SBA) levels therefore serve as sensitive indicator of liver disease [4–10]. Because of the minor daily meal-based fluctuations and their excessive levels during liver-associated pathologies, SBAs have been suggested to play a more prominent metabolic role exceeding the one of emulsifying nutrients [2,11].

Indeed, bile acids have recently emerged as versatile signalling compounds endowed with systemic endocrine function

ELSEVIER

Molecular and Cell Biology

[2]. Bile acids are ligands of several nuclear hormone receptors such as farnesoid X receptor (FXR) and G-protein-coupled receptors (GPCR) such as TGR5 through which they activate diverse signalling pathways that regulate triglyceride, cholesterol, glucose and energy homeostasis as well as their own synthesis, enterohepatic circulation, inflammation and liver regeneration [2,11]. In particular, bile acid-mediated activation of TGR5 coordinates renal clearance of bile acids, thereby preventing toxic bile acid overload [11,12]. In addition, pro-inflammatory mediators induce the production of hepatocyte growth factor (HGF), which has a potent cytoprotective impact on hepatocytes, triggers their proliferation and stimulates migration and proliferation of activated hepatic stem cells into the liver parenchyma, where the cells differentiate into mature hepatocytes [13–15].

Liver diseases are particularly difficult to diagnose as latent inflammations leading to critical fibrosis, irreversible cirrhosis and organ failure may go unnoticed as they fail to trigger any symptoms or significant discomfort [16,17]. To date, liver transplantation is the major treatment option for late-stage liver diseases [1]. However, because of the shortage of donor livers, as well as the significant risk associated with transplantation and life-long immunosuppression, a genetically engineered cell-based theranostic liver-protection device combining precise diagnosis of acute liver injuries with targeted therapeutic or hepatoprotective interventions may represent an attractive alternative.

Capitalizing on SBAs as a well-established biomarker for a wide variety of liver-associated pathologies [4–10], TGR5 as a liver injury-specific bile acid sensor and HGF as a promising protein therapeutic validated in human clinical trials [18–21], we have functionally linked these components using a synthetic biology-based design strategy to create a closed-loop synthetic gene network that detects the onset of liver injury, initiates HGF-mediated liver regeneration and prevents liver failure.

Materials and methods

Components of the liver-protection device

Comprehensive design and construction details for all expression vectors are provided in Table 1. The key components of the liver-protection device includes pBP2 for constitutive low-level expression of the human bile acid receptor TGR5 ($P_{hCMV*-1}$-TGR5-pA) and pPB5, which produces human hepatocyte growth factor in a bile acid-responsive TGR5-dependent manner (P_{CREm}-HGF-pA).

Cell culture and transfection

Human embryonic kidney cells (HEK-293, ATCC: CRL-11268 [HEK-293T]), baby hamster kidney cells (BHK-21, ATCC: CCL-10), human fibrosarcoma cells (HT-1080, ATCC: CCL-121) and telomerase-immortalised human mesenchymal stem cells (hMSC-TERT, [22]) were cultured in Dulbecco's modified Eagle's medium (DMEM; Invitrogen, Basel, Switzerland; cat. no. 52100-39) supplemented with 10% (v/v) fetal bovine serum (FBS; Sigma-Aldrich, Munich, Germany; cat. no. F7524, lot no. 022M3395) or 10% (v/v) charcoal-stripped FBS (cFBS, Sigma-Aldrich; cat. no. F6765, lot no. 13C443) and 1% (v/v) penicillin/streptomycin solution (Sigma-Aldrich; cat. no. P4333). Wild-type Chinese hamster ovary cells (CHO-K1, ATCC: CCL-61) were cultured in ChoMaster® HTS (Cell Culture Technologies, Gravesano, Switzerland; cat. no. HTS-8) supplemented with 5% (v/v) FBS and 1% penicillin/streptomycin solution. Freestyle™ 293-F suspension cells (Life Technologies, Carlsbad, CA; cat. no. R79007) were cultivated in FreeStyle™ 293 Expression Medium (Life Technologies; cat. no. 12338018) supplemented with 1% penicillin/streptomycin solution and grown in 12 well plates or shake flasks placed on an orbital shaker (IKA KS 260 basic; IKA-Werke GmbH, Staufen im Breisgau, Germany; cat. no. 0002980200) set to 100–150 rpm. All cell types were cultivated at 37 °C in a humidified atmosphere containing 5% CO_2. All cell lines were transfected using an optimized polyethyleneimine (PEI)-based protocol [23]. For transfection of CHO-K1, HEK-293, BHK-21, HT-1080 and hMSC-TERT, 5×10^4 cells seeded per well of a 24 well plate 20 h before transfection were incubated with a transfection solution containing 0.55 μg plasmid DNA (for co-transfections equal amounts of plasmid DNA was used) and 2.2 μl of PEI (polyethyleneimine; MW40,000, stock solution 1 μg/μl in ddH$_2$O; Polysciences, Eppelheim, Germany; cat. no. 24765-2). For transfection of suspension FreeStyle™ 293-F cells, 1×10^6 cells seeded per well of a 12 well plate 1 h before transfection were incubated with a transfection solution containing 1.1 μg plasmid DNA and 4.4 μl PEI (1 μg/μl). The DNA/PEI transfection solution was mixed with 50 μl 150 mM NaCl, incubated for 15 min at 22 °C and added dropwise to the cells. Cell concentrations were profiled with a CASY® Cell Counter and Analyser System Model TT (Roche Diagnostics GmbH, Mannheim, Germany).

Animal experiments

Intraperitoneal genetically engineered cell implants were produced by encapsulating pHY74/pSP16 ($P_{hCMV*-1}$-eYFP-pA/P_{CREm}-SEAP-pA)-, pPB2/pSP16 ($P_{hCMV*-1}$-TGR5-pA/P_{CREm}-SEAP-pA)-, pPB2/pPB5 ($P_{hCMV*-1}$-TGR5-pA/P_{CREm}-HGF-pA)- and pPB7 (P_{hCMV}-HGF-pA)-transgenic HEK-293 cells into coherent alginate-poly-(L-lysine)-alginate beads (400 μm; 200 cells/capsule) using an Inotech Encapsulator Research Unit IE-50R (Buechi Labortechnik AG, Flawil, Switzerland) set to the following parameters: 25 ml syringe operated at a flow rate of 450 units, 200 μm nozzle with a vibration frequency of 1,020 Hz and 1.1 kV for bead dispersion, stirrer speed at 4.5 units. 8 week-old female OF1 mice (oncins France souche 1, Charles River Laboratory, Lyon, France) were intraperitoneally injected with $2–5 \times 10^6$ cells (700 μl DMEM containing $1–2.5 \times 10^4$ capsules, 200 cells/capsule) and were treated with bile acids (cholic acid [0–160 mg/kg] or tauroursodeoxycholic acid [0–160 mg/kg], twice-daily intraperitoneal injections of 0–80 mg/kg; cholic acid [0–160 mg/kg] or deoxycholic acid [0–80 mg/kg], twice-daily intravenous injections of 0–80 mg/kg; cholic acid [0–160 mg/kg], tauroursodeoxycholic acid [0–40 mg/kg] or deoxycholic acid [0–160 mg/kg], twice or fourth-daily oral administration of 0–40 mg/kg), hepatotoxicants (1-Naphtyl isothiocyanate [75 mg/kg] or carbon tetrachloride [1 ml/kg], single oral dose) or olive oil (8 ml/kg, single oral dose). Blood samples were collected 48 h after treatment and the serum was isolated using BD Microtainer® SST tubes according to the manufacturer's instructions (centrifugation for 5 min at 10,000 g; Becton Dickinson, Plymouth, UK; cat. no. 365967). All mice were kept on a standard diet (5 kcal % fat; Janvier S.A.S., Le Genest-Saint-Isle, France) unless indicated otherwise. After completion of the experiments, the animals were sacrificed and their liver collected for histological analysis. All experiments involving animals were performed according to the directives of the European Community Council (2010/63/EU), approved by the French Republic (no. 69266309 and no. 69266310; project no. DR2013-01 (v2)) and carried out by Ghislaine Charpin-El Hamri and Marie Daoud-El Baba at the University of Lyon, Institut Universitaire de Technologie (IUTA), F69622 Villeurbanne Cedex, France.

Histology

Two days after implantation of microencapsulated pPB2/pPB5-, pPB2/pSP16- or pPB7-transgenic cells and subsequent oral administration of a single dose of ANIT or olive oil, the mice were sacrificed and their livers were explanted. Five representative liver slices (2–3 mm thick) of each animal were fixed in 0.1 M sodium cacodylate buffer (pH7.4, 540 mOsm; Sigma-Aldrich, USA, cat. no. CO250) containing 2.5% (v/v) glutaraldehyde (AGAR Scientific Ltd., Stansted, UK, cat. no. R1010) and stored at 4 °C until further processing. Tissue blocks of approximately 1 mm^3 were cut, rinsed in 0.1 M sodium cacodylate buffer (3 × 10 min, pH 7.4, 340 mOsm) and post-fixed in 0.1 M sodium cacodylate buffer containing 1% (w/v) osmium tetroxide (Electron Microscopy Sciences, Hatfield PA, USA cat. no. 19100) at 4 °C for 2 h. The samples were then washed in 0.1 M sodium cacodylate buffer (3 × 10 min, pH 7.4, 340 mOsm), dehydrated by serial incubation in ddH$_2$O containing increasing concentrations of ethanol (70%, 80%, 90%, 96%, 99%, 100%) and embedded in EPON 812 (Fluka, Sigma-Aldrich, Buchs, CH, cat. nos. 45245-45347). One μm thick liver sections were prepared using glass knives, stained with toluidine blue (Fluka, Buchs, CH, cat. no. 89640) and analysed by light microscopy (100×–630× magnification, Imager M2, Zeiss, Jena, De). At least five animals per treatment group were analysed.

Statistics

Results are expressed as mean ± SEM. Statistical significance of datasets was evaluated by a two-tailed, unpaired Student's t test using Graphpad Prism V6.0d. $p < 0.05$ was considered significant.

Research Article

Table 1. Plasmids used and designed in this study.

Plasmid	Description and cloning strategy	Reference or source
pBABE-puro	Retroviral expression vector.	[58]
pcDNA3.1(+)	Mammalian expression vector (P_{hCMV}-MCS-pA).	Life Technologies, Carlsbad, CA
pEYFP-C1	Constitutive EYFP expression vector (P_{hCMV}-EYFP-pA).	Clontech, Mountain View, CA
pSEAP2-Control	Constitutive SEAP expression vector (P_{SV40}-SEAP-pA).	Clontech, Mountain View, CA
pCMV-SPORT6	Mammalian expression vector (P_{hCMV}-MCS-pA).	Life Technologies, Carlsbad, CA
pBABE-puro HGF	pBABE-puro containing full-length HGF cDNA.	[59]
pTGR5	pCMV-SPORT6 containing a constitutive TGR5 expression unit (P_{hCMV}-TGR5-pA).	GenBank: BC033625
pCK53	P_{CRE}-driven SEAP expression vector (P_{CRE}-SEAP-pA).	[60]
pMF111	$P_{hCMV^{*-1}}$-driven SEAP expression vector ($P_{hCMV^{*-1}}$-SEAP-pA).	[61]
MKp37	Constitutive TetR-ELK1 expression vector (P_{hCMV}-TetR-ELK1-pA).	[62]
pSP16	P_{CREm}-driven SEAP expression vector (P_{CREm}-SEAP-pA).	[63]
pHY57	P_{NFAT}-driven shGLP1 expression vector (P_{NFAT}-shGLP1-pA).	[31]
pHY67	P_{CRE}-driven shGLP1 expression vector (P_{CRE}-shGLP1-pA).	Ye et al., unpublished
pHY74	$P_{hCMV^{*-1}}$-driven EYFP expression vector ($P_{hCMV^{*-1}}$-EYFP-pA). EYFP was PCR-amplified from pEYFP-C1 using oligonucleotides OHY163 (5'-gcgccgacgaattcGCCACCATGGTGAGCAAGGGCGAGGAGCTGTTCACC-3') and OHY164 (5'-cacgcacgaagcttTTACTTGTACAGCTCGTCCATGCC-3'), restricted with EcoRI/HindIII and cloned into the corresponding sites (EcoRI/HindIII) of pMF111.	This work
pPB2	$Ph_{CMV^{*-1}}$-driven TGR5 expression vector ($P_{hCMV^{*-1}}$-TGR5-pA). TGR5 was excised from pCMV-SPORT6-TGR5 using EcoRI/HindIII and cloned into the corresponding sites (EcoRI/HindIII) of pMF111.	This work
pPB5	P_{CREm}-driven HGF expression vector (P_{CREm}-HGF-pA). P_{CREm} was PCR-amplified from pSP16 using oligonucleotides OPB29 (5'-TCTTACGCGTGCTAGCAGC-3') and OPB39 (5'-gcgaattcgcgaTTTACCAACAGTACCGGATT-3'), restricted with NheI/NruI and cloned into the corresponding sites (NheI/NruI) of pPB6.	This work
pPB6	P_{CRE}-driven HGF expression vector (P_{CRE}-HGF-pA). HGF was PCR-amplified from pBABE-puro HGF using oligonucleotides OPB33 (5'-gcttcgaatcgcgaATTCGCCCACCATGTGGGTGACCAAA-3') and OPB32 (5'-cgactctagaTTCAGCTATGACTGTGGTAC-3'), restricted with NruI/XbaI and cloned into the corresponding sites (NruI/XbaI) of pCK53.	This work
pPB7	Constitutive HGF expression vector (P_{hCMV}-HGF-pA). HGF was PCR-amplified from pBABE-puro HGF using oligonucleotides OPB50 (5'-cgcggatccACCATGTGGGTGACCAAA-3') and OPB32 (5'-cgactctagaTTCAGCTATGACTGTGGTAC-3'), restricted with BamHI/XbaI and cloned into the corresponding sites (BamHI/XbaI) of pcDNA3.1(+).	This work
pPB8	P_{CREm}-driven shGLP1 expression vector (P_{CREm}-shGLP1-pA). P_{CREm} was excised from pSP16 using KpnI/EcoRI and cloned into the corresponding sites (KpnI/EcoRI) of pHY57.	This work

CRE, cAMP-response element; CREm, modified cAMP-response element; ELK1, ETS domain-containing transcription factor; ETS, E26 transformation-specific or E-twenty-six transcription factor family; EYFP, enhanced yellow fluorescent protein; HGF, human hepatocyte growth factor; MCS, multiple cloning site; NFAT, nuclear factor of activated T cells; pA, polyadenylation signal; P_{CRE}, CRE containing synthetic mammalian promoter; P_{CREm}, modified P_{CRE} variant; PCR, polymerase chain reaction; P_{hCMV}, human cytomegalovirus immediate early promoter; $P_{hCMVmin}$, minimal version of P_{hCMV}; $P_{hCMV^{*-1}}$, tetracycline-responsive promoter (tetO$_7$-$P_{hCMVmin}$); P_{NFAT}, synthetic mammalian promoter containing a NFAT-response element; P_{SV40}, simian virus 40 promoter; TetR, Escherichia coli Tn10-derived tetracyclinedependent repressor of the tetracycline resistence gene; tetO$_7$, TetR-specific heptameric operator sequence; TetR-ELK1, TetR-ELK1 fusion protein; SEAP, human placental secreted alkaline phosphatase; shGLP1, short human glucagon-like peptide 1; TGR5, human bile acid receptor (GenBank: BC033625) also known as GPBAR1 (G protein–coupled bile acid receptor 1) or M-BAR (membrane-type receptor for bile acids).
Oligonucleotides: Restriction endonuclease-specific sites are in italics and annealing base pairs are indicated in capital letters.

Results

Design and characterization of the synthetic mammalian bile acid sensor

Bile acid-inducible activation of the human GPCR TGR5 triggers an intracellular signal transduction cascade involving $G_{\alpha S}$-protein-mediated activation of the plasma membrane-bound adenylate cyclase, which converts ATP into the second messenger cyclic AMP (cAMP) [2]. Upon rewiring of the intracellular cAMP surge via cAMP-dependent phosphokinase A (PKA)-mediated activation of the cAMP-response element binding protein (CREB1) to CREB1-specific synthetic promoters (P_{CRE}, P_{CREm}) containing cAMP-response elements (CRE), bile acid levels could be directly coupled to expression of a specific target gene (Fig. 1A).

Initial experiments using different expression platforms (pTGR5, P_{hCMV}-TGR5-pA; pPB2, $P_{hCMV^{*-1}}$-TGR5-pA) showed that TGR5 was efficiently transcribed (Supplementary Fig. 1A), produced (Supplementary Fig. 1B) and triggered a bile acid (cholic acid)-dependent cAMP surge (Supplementary Fig. 1C) in mammalian cells. Since pPB2 provided optimal cholic acid-triggered transgene expression when co-transfected with the reporter construct pCK53 (P_{CRE}-SEAP-pA$_{SV40}$; SEAP, human placental secreted alkaline phosphatase) we used it as the preferred TGR5 expression vector in all follow-up experiments (Fig. 1B). In order to further improve tightness of the bile acid sensor we created P_{CREm} (pSP16; P_{CREm}-SEAP-pA), a modified P_{CRE}, that showed similar bile acid-responsive induction kinetics and a comparable dynamic range but exhibited lower leakiness and lower maximum expression levels compared to P_{CRE} (Fig. 1C–1D). The bile
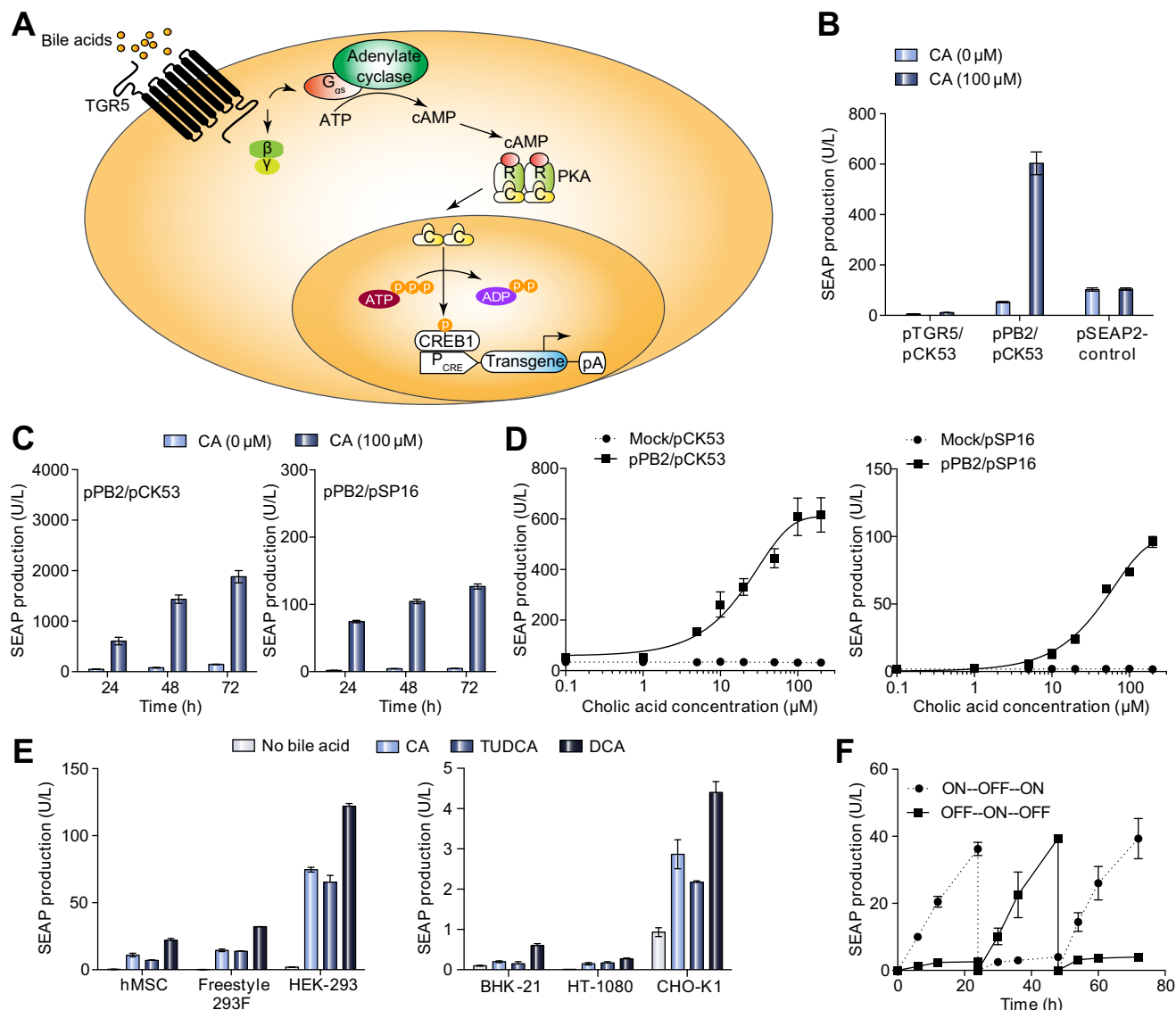
Fig. 1. Design and characterization of the synthetic mammalian bile acid sensor. (A) Design of a synthetic bile acid-triggered signalling cascade. The G protein-coupled bile acid receptor 1 (TGR5) senses extracellular bile acids and triggers $G\alpha_s$-mediated activation of adenylate cyclase, which converts ATP to cyclic AMP (cAMP). cAMP binds the regulatory subunits of protein kinase A (PKA), whose catalytic subunits translocate into the nucleus where they phosphorylate the cAMP-responsive binding protein 1 (CREB1). Subsequently, CREB1 binds and activates target gene transcription from synthetic promoters P_{CRE} engineered to contain different CREB1 response elements (CRE). (B) Cholic acid-inducible transgene expression in HEK-293 cells using different TGR5 expression vectors. HEK-293 cells were co-transfected with pCK53 (P_{CRE}-SEAP-pA; 100 ng) and either pTGR5 (P_{hCMV}-TGR5-pA; 1000 ng) or pPB2 ($P_{hCMV*-1}$-TGR5-pA; 1000 ng) and cultivated in the presence or absence CA (100 μM). HEK-293 cells transfected with pSEAP2-Control (P_{SV40}-SEAP-pA; 100 ng) were used as control. SEAP levels in the culture supernatants were scored after 24 h. Data presented are mean ± SD, n ⩾3. (C) SEAP expression kinetics. HEK-293 cells were co-transfected with pPB2 ($P_{hCMV*-1}$-TGR5-pA; 1000 ng) and either pCK53 (P_{CRE}-SEAP-pA; 100 ng) or pSP16 (P_{CREm}-SEAP-pA; 100 ng) and cultivated for 72 h in the presence or absence of CA (100 μM). SEAP levels in the culture supernatants were scored every 24 h. Data presented are mean ± SD, n ⩾3. (D) Dose-dependent SEAP expression. HEK-293 cells were co-transfected with pPB2 ($P_{hCMV*-1}$-TGR5-pA; 1000 ng) and either pSP16 (P_{CREm}-SEAP-pA; 100 ng) or pCK53 (P_{CRE}-SEAP-pA; 100 ng) and cultivated for 24 h in the presence of different CA concentrations (0–200 μM) before SEAP levels in the culture supernatants were scored. Data presented are mean ± SD, n ⩾3. (E) Bile acid-inducible SEAP expression in different mammalian cell lines. hMSC, Freestyle 293F, HEK-293, BHK-21, HT-1080 and CHO-K1 cells were co-transfected with pPB2/pSP16 (1000 ng/100 ng) and cultivated in medium containing different bile acid derivatives (CA: 100 μM; tauroursodeoxycholic acid TUDCA: 100 μM; deoxycholic acid DCA: 100 μM for hMSC, BHK-21, HT-1080, CHO-K1 and HEK-293, 10 μM for Freestyle 293F). SEAP levels in the culture supernatant were scored 24 h after addition of bile acids. Data presented are mean ± SD, n ⩾3. (F) Reversibilty of cholic acid-inducible SEAP expression. pPB2/pSP16-transgenic HEK-293 cells were cultivated in the presence (ON, for 6 h) or absence (OFF) of CA (100 μM). Every 24 h, the CA status of the culture was reversed and SEAP production was profiled for up to 72 h. Data presented are mean ± SD, n ⩾3. (This figure appears in colour on the web.)

acid sensor was functional in different pPB2-/pSP16-co-transfected mammalian cell lines including human ones, such as, suspension cell lines and stem cells, suggesting that the synthetic signalling cascade was broadly applicable (Fig. 1E). As expected, possible differences in availability and compatibility of the endogenous signal transduction components with TGR5-mediated input resulted in a wide range of induction factors [24]. Since HEK-293 showed the best bile acid-triggered expression performance, this cell line was chosen for all further experiments (Fig. 1E).

Molecular and Cell Biology

Research Article

Detailed characterization of pPB2-/pSP16-co-transfected HEK-293 cells showed that (i) the bile acid sensor neither reduced cell viability (Supplementary Fig. 2A) nor maximum SEAP production levels over the entire clinically relevant bile acid concentration range (Supplementary Fig. 2B), (ii) that bile acid-triggered target gene expression switches correlated with intracellular cAMP levels (Supplementary Fig. 1C), (iii) that the TGR5-to-P$_{CREm}$ signalling could be interrupted by the PKA inhibitor H-89 confirming the exclusive rewiring (Supplementary Fig. 2C) and, most importantly, (iv) that physiological concentrations of ligands targeting HEK-293's endogenous GPCRs sharing the cAMP pathway did not interfere with the bile acid sensor (Supplementary Fig. 2D), which corroborates the specificity of the biosensor and supports previous reports that ectopic expression of GPCRs in mammalian cells attenuates ligand-specific activation of endogenous GPCRs in the same cell, likely by titrating away the endogenous G-protein pool [25].

Bile acid-inducible transgene expression in mammalian cells

In order to be functional as part of a higher-order closed-loop liver-protection device *in vivo* the bile acid sensor has to (i) be sufficiently sensitive to detect the major bile-composing native and modified bile acids within their clinically relevant concentrations range, (ii) show rapid response times and induction kinetics to manage protective and curative therapeutic responses preventing liver failure, (iii) provide bile acid dose-dependent therapeutic transgene expression to coordinate the level of liver injury to the level of therapeutic intervention and (iv) to deliver reversible control dynamics which enable the design of a closed-loop gene circuit that constantly adapts the therapeutic expression dosing to the course of the liver disease and protects against liver failure through enhanced regeneration.

Cholic acid (CA), chenodeoxycholic acid (CDCA), deoxycholic acid (DCA), lithocholic acid (LCA) including their conjugated (tauro- and glyco-) isoforms represent over 95% of the bile acids found in the human serum [26]. Tauroursodeoxycholic acid (TUDCA), a major bile acid in the serum of bears with only trace amounts found in human and mouse sera, has been associated with potent cytoprotective and antidiabetic activities [26–30]. Human cells containing the bile acid sensor (pPB2/pPS16) were able to detect all (non-)conjugated human and bear bile acids within their clinically relevant concentration range and produced a dose-dependent reporter gene expression profile (Supplementary Fig. 3A) with rapid induction kinetics (Supplementary Fig. 3B). As exemplified using CA as trigger bile acid, bile acid sensor-driven expression kinetics could be precisely programmed by the bile acid exposure time (Supplementary Fig. 3C), which confirmed the rapid response time and induction kinetics of the bile acid sensor. In addition, bile acid sensor-driven reporter gene expression was reversible and showed reproducible induction kinetics when repeatedly switched ON and OFF following addition and withdrawal of bile acids (Fig. 1F).

Bile acid-inducible protein production in serum-free suspension cultures

Dose- and time-specific control of product gene expression in bioreactors requires availability of gene switches that are responsive to trigger cues which are generally regarded as safe (GRAS) and licensed by food and healthcare authorities. Desoxycholic

acid is a GRAS compound that, is clinically licensed by the Food and Drug Administration (FDA) and approved in many countries as an emulsifier for the food industry and could therefore be considered as a product gene expression trigger in a biopharmaceutical manufacturing setting. We have therefore tested desoxycholic acid as trigger compound for the timely induction of the short human glucacon-like peptide 1 (shGLP1), a long-acting insulinogenic hormone engineered for the treatment of type 2 diabetes mellitus [31], in HEK-293-derived serum-free suspension cultures which is currently considered for the production of viral particles for vaccines and gene therapy [32]. In standard bioreactor operation, shGLP1-expression of HEK-293 cells transgenic for pPB2 and either pPB8 (P$_{CREm}$-shGLP1-pA) (Fig. 2A) or pHY67 (P$_{CRE}$-shGLP1-pA) (Fig. 2B) was tightly repressed until addition of a specific amount of desoxycholic acid which programmed the shGLP1 expression kinetics and final titer of the production culture to specific levels (Fig. 2).

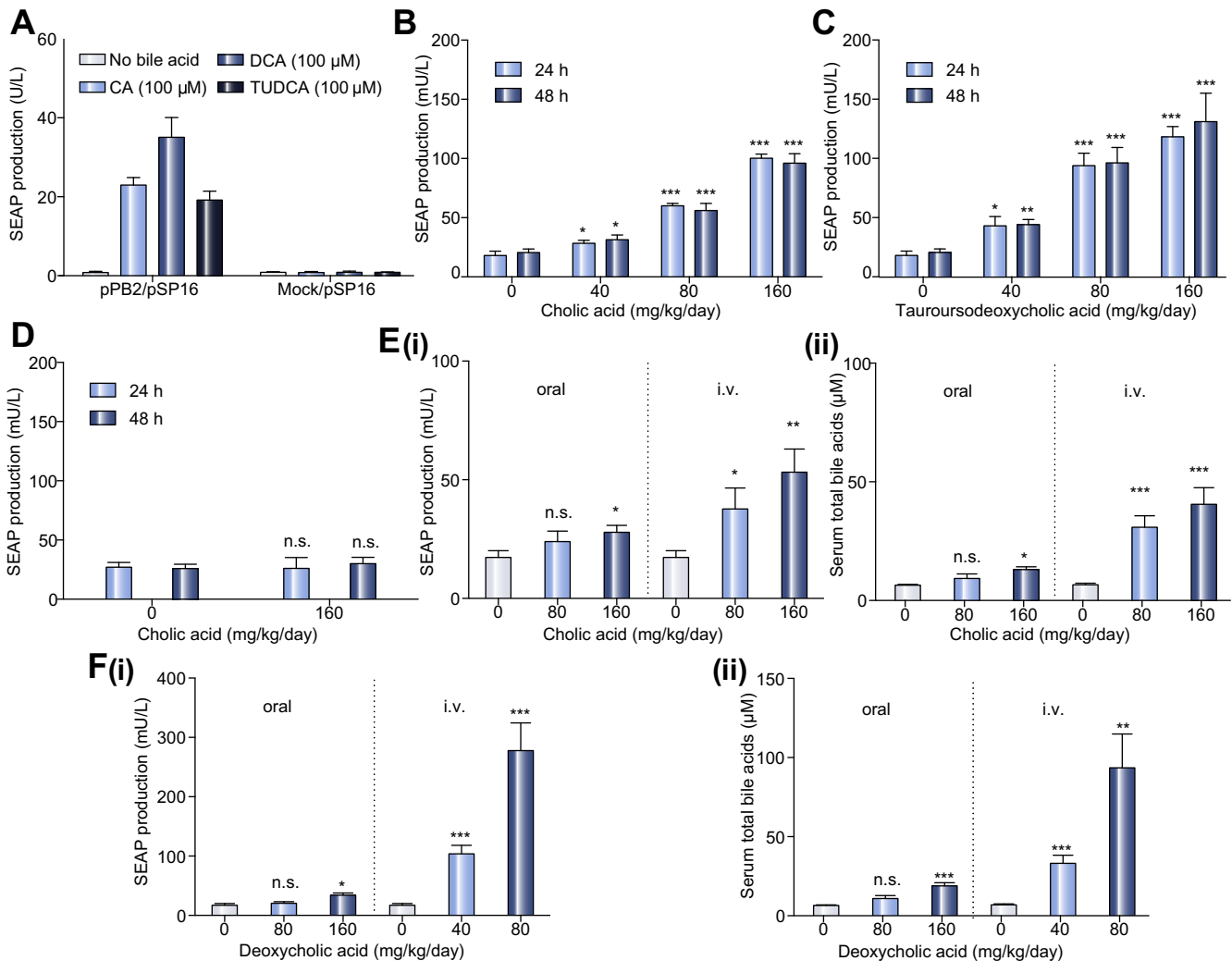*Bile acid-inducible transgene expression in mice*

To validate bile acid-inducible transgene expression *in vivo*, we microencapsulated pPB2/pSP16-transgenic HEK-293 cells into clinically validated, semi-permeable and immunoprotective
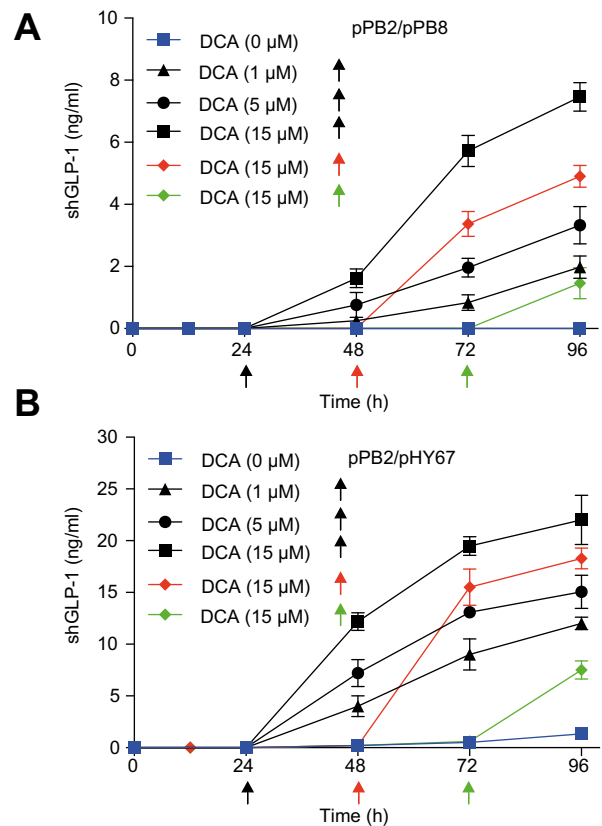
Fig. 2. DCA-triggered shGLP-1 production in bioreactors. (A) shGLP-1 production kinetics of pPB2/pPB8 (TGR5/P$_{CREm}$-shGLP1)- or (B) pPB2/pHY67 (TGR5/P$_{CRE}$-shGLP1)- transgenic Freestyle 293F suspension cells grown in bioreactors triggered by addition of 1 μM, 5 μM or 15 μM DCA at 24 h, 48 h or 72 h. Control bioreactors were run in the absence of DCA. shGLP1 production was profiled in the culture medium at indicated time points. Data presented are mean ± SD, n = 3. DCA, deoxycholic acid. (This figure appears in colour on the web.)

Molecular and Cell Biology

alginate-poly-(L-lysine)-alginate beads (Fig. 3A) and implanted them into the peritoneum of mice where they become vascularized and connected to the animal's bloodstream [33]. When mice received increasing doses of the clinically licensed drugs CA (Cholbam®) (Fig. 3B) or tauroursodenoxycholic acid (TUDCA) (Fig. 3C) by intraperitoneal injection, the implanted genetically engineered cells detected circulating bile acid levels by bile acid dose-dependent TGR5-mediated expression of SEAP (Fig. 3D),

which reached the bloodstream and could be profiled in the peripheral circulation of the animals (Fig. 3B, C). Likewise, the SEAP levels in the bloodstream of treated animals could also be modulated by intravenous injection as well as oral administration of CA (Fig. 3E) and deoxycholic acid (Fig. 3F), confirming that the cell implant is fully integrated in the systemic circulation of the host organism and sensitive to physiologically relevant bile acid concentrations.

Fig. 3. Bile acid-inducible transgene expression in mice. (A) SEAP induction profiles of microencapsulated TGR5/P$_{CREm}$-SEAP HEK-293 cells *in vitro*. HEK-293 cells were co-transfected with pSP16 (P$_{CREm}$-SEAP-pA) and either pPB2 (P$_{hCMV*-1}$-TGR5-pA) or pHY74 (P$_{hCMV*-1}$-eYFP-pA) and microencapsulated into alginate-poly-(L-lysine)-alginate beads. 5×10^3 capsules (200 cells/capsule) were cultivated in the presence or absence of CA (100 μM), deoxycholic acid (DCA; 100 μM) or tauroursodeoxycholic acid (TUDCA; 100 μM). SEAP levels in the culture supernatants were scored after 24 h. Data presented are mean ± SD, n ⩾3. (B, C) Dose-dependent bile acid-inducible SEAP expression in mice. Wild-type mice were intraperitoneally implanted with microencapsulated TGR5/P$_{CREm}$-SEAP (pPB2/pSP16, 2×10^6 cells, 1×10^4 capsules, 200 cells/capsule)-transgenic HEK-293 cells and received intraperitoneal injections of different daily doses of CA (B) or tauroursodeoxycholic acid (C). SEAP levels in the bloodstream of treated animals were quantified 24 h and 48 h after the first bile acid administration. The data are shown as the mean ± SEM, statistics by two-tailed *t* test, n = 8 mice. *p <0.05, **p <0.01, ***p <0.001 *vs.* control. (D) Negative control group. Wild-type mice were intraperitoneally implanted with microencapsulated pHY74/pSP16-transfected HEK-293 control cells (2×10^6 cells, 1×10^4 capsules, 200 cells/capsule) and received intraperitoneal injections of different daily doses of CA. Serum SEAP levels were quantified in the bloodstream of treated animals after 24 h and 48 h. The data are shown as the mean ± SEM, statistics by two-tailed *t* test, n = 6 mice. n.s. (not significant) p >0.05 *vs.* control. (E, F) Dose-dependent bile acid-inducible SEAP expression in mice. Wild-type mice were intraperitoneally implanted with microencapsulated pPB2/pSP16-transfected HEK-293 cells (2×10^6 cells, 1×10^4 capsules, 200 cells/capsule) and received different daily intravenous or oral doses of cholic acid (CA) (E) or deoxycholic acid (DCA) (F). (i) SEAP and (ii) total bile acid levels in the bloodstream of treated animals were quantified 48 h after the first bile acid administration. The data are shown as the mean ± SEM, statistics by two-tailed *t* test, n = 6 mice. n.s. (not significant) p >0.05, *p <0.05, **p <0.01, ***p <0.001 *vs.* control.

Molecular and Cell Biology

Research Article

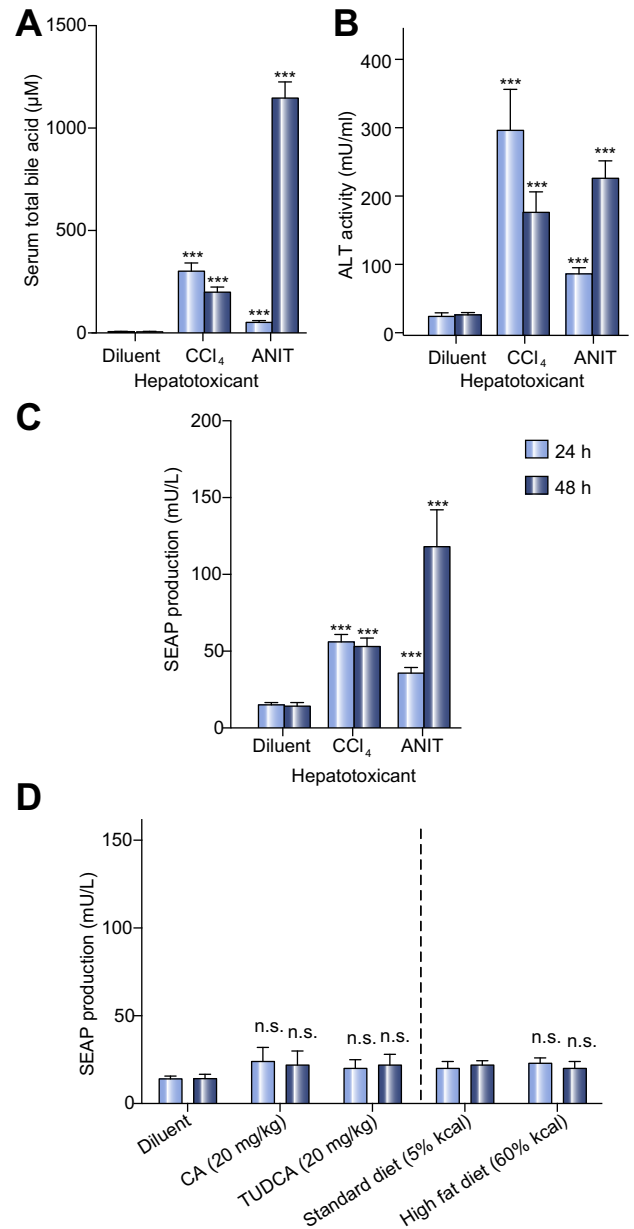*The bile acid sensor detects acute liver injuries in mice*

The enterohepatic circulation maintains serum bile acid (SBA) levels below 20 μM in man and mice (Fig. 4A) [4–10]. Liver injuries result in imbalances of the enterohepatic circulation leading to acute and chronically increased SBA concentrations (>20 μM in humans), which correlate with excessive blood alanine aminotransferase (ALT) levels (>30–40 U/L in humans and mice) that serves as the gold standard biomarker of liver injury [34,35]. Carbon tetrachloride (CCl$_4$) and alpha-naphthylisothiocyanate (ANIT) are the reference compounds to replicate human drug-induced hepatotoxicity in mice as they either mediate direct destruction of hepatocytes or induce cholestasis by damaging biliary epithelial cells, respectively [36,37]. When mice implanted with pPB2/pSP16-transgenic HEK-293 cells received oral doses of the hepatotoxicants CCl$_4$ (1 ml/kg) or ANIT (75 mg/kg), SBA and ALT levels immediately rose into the critical range (Fig. 4A, B). The acute liver injury was detected and processed by the implanted genetically engineered cell-based bile acid sensor which coordinated the production, secretion and release of the reporter protein SEAP into the bloodstream of treated animals (Fig. 4C). The biosensor was insensitive to the minor diet-induced SBA fluctuations (Fig. 4D) as well as oral dietary-supplement doses of CA, deoxycholic acid and TUDCA that are expected to be cleared by the first-pass effect of a healthy liver (Fig. 3E, Fig. 3F, Fig. 4D). Therefore, the sensitivity of the genetically engineered cell-based bile acid sensor is well suited to exclusively detect pathologic SBA levels in the event of an acute liver injury.

## Validation of a self-sufficient closed-loop liver-protection device in mice

Advanced theranostic gene networks combine precise diagnosis of a pathologic situation with targeted therapeutic intervention in a closed-loop control circuit which prevents or cures a specific disease [38]. Therefore, the design of a liver-protection device requires functional interconnection of the bile acid sensor with expression of a therapeutic protein that can prevent liver failure and restore liver function. The human HGF, a secreted protein associated with tissue protection, organ regeneration and wound healing, has recently come into the limelight for the treatment of various organ injuries. Unfortunately, the short half-life (<5 min, [39–41]) of HGF in circulation would require repeated high-dose injections which exacerbates its use as a biopharmaceutical for the time being. However, human clinical trials have shown that *in situ* production of HGF using a gene therapy approach may provide the full scope of HGF's therapeutic potential [18–21].

We have therefore linked SBA-triggered activation of TGR5 (pPB2, P$_{hCMV^{*}-1}$-TGR5-pA) to P$_{CREm}$-driven expression of HGF (pPB5, P$_{CREm}$-HGF-pA). *In vitro* validation of pPB2-/pPB5-transgenic HEK-293 cells confirmed that the genetically engineered cells were able to secrete clinically relevant levels (Supplementary Fig. 4A) of bioactive HGF (Supplementary Fig. 4B) in response to liver injury-associated bile acid concentrations. When implanting the same cells into mice, the animals were protected from ANIT-induced liver failure and showed significantly reduced blood values of ALT activity (Fig. 5A), SBA levels (Fig. 5B) or bilirubin concentration (Fig. 5C), while the serum levels of all these liver injury-specific biomarkers were dramatically increased in mice treated with placebo implants. Most importantly, the liver-protection device drove high-level HGF

Fig. 4. The bile acid sensor detects acute liver injuries in mice. (A, B) Chemically induced hepatotoxicity in mice. Wild-type mice were implanted with microencapsulated TGR5/P$_{CREm}$-SEAP (pPB2/pSP16, 2×10^6 cells, 1×10^4 capsules, 200 cells/capsule)-transgenic HEK-293 cells and received a single oral dose of 1 ml/kg CCl$_4$ (carbon tetrachloride) or 75 mg/kg ANIT (alpha-naphthylisothiocyanate) diluted or dissolved in olive oil (diluent), and (A) total serum bile acid levels or (B) alanine aminotransferase (ALT) activity was measured after 24 h and 48 h. The data are shown as the mean ± SEM, statistics by two-tailed *t* test, n = 8 mice. ***p <0.001 *vs.* control. (C) Hepatotoxicity-mediated SEAP expression in mice. SEAP levels in the bloodstream of treated mice shown in (A, B) were quantified after 24 h and 48 h. The data are shown as the mean ± SEM, statistics by two-tailed *t* test, n = 8 mice. ***p <0.001 *vs.* control. (D) Diet insensitivity of the liver-protection device. Wild-type mice were implanted with microencapsulated TGR5/P$_{CREm}$-SEAP (pPB2/pSP16, 2×10^6 cells, 1×10^4 capsules, 200 cells/capsule)-transgenic HEK-293 cells and kept on standard (5% kcal fat) or high-fat diets (60% kcal fat, Research Diets, cat. no. D12492i) or received twice-daily oral doses of either cholic acid (CA; 20 mg/kg) or tauroursodeoxycholic acid (TUDCA; 20 mg/kg) before blood SEAP levels were quantified after 24 h and 48 h. The data are shown as the mean ± SEM, statistics by two-tailed *t* test, n = 8 mice. n.s. (not significant) p >0.05 *vs.* control.
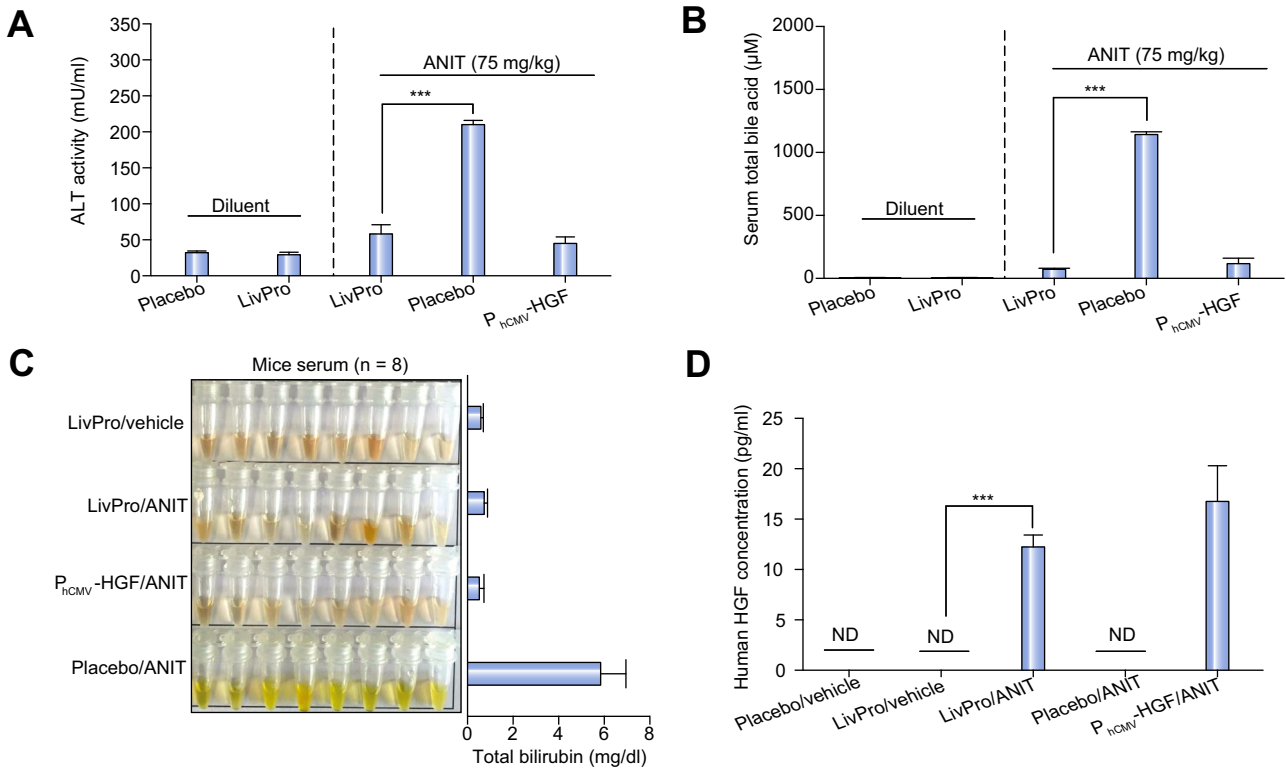
Fig. 5. Self-sufficient SBA-mediated activation of HGF expression in animals treated with the liver-protection device. (A-D) Animals received either genetically engineered cell implants (5×10^6 cells, 25000 capsules, 200 cells/capsule) containing the liver-protection device (pPB2/pPB5; P_{hCMV^*-1}-TGR5-pA/P_{CREm}-HGF-pA), a placebo device (pPB2/pSP16; P_{hCMV^*-1}-TGR5-pA/P_{CREm}-SEAP-pA; negative control) or a constitutive HGF expression unit (pPB7; P_{hCMV}-HGF-pA; positive control) and were treated with a single dose of either ANIT (75 mg/kg in olive oil) or the diluent olive oil (8 ml/kg). (A) Alanine aminotransferase (ALT) activity, (B) total serum bile acid levels and (C) bilirubin levels in sampled mouse serum were measured 48 h after oral administration of hepatotoxicants. The data are shown as the mean ± SEM, statistics by two-tailed t test, n = 8 mice. ***p <0.001. (D) Serum HGF concentration of corresponding treatment groups shown in (A–C). The data are shown as the mean ± SEM, statistics by two-tailed t test, n = 8 mice. ***p <0.001. n.d.: not detected (detection limit 3 pg/ml). LivPro, liver-protection device (pPB2/pPB5). (This figure appears in colour on the web.)

production exclusively following ANIT-triggered increase of SBA levels (Fig. 5D). Histological analysis of the liver of treated animals corroborated the finding that the liver-protection device was able to prevent drug-induced hepatotoxicity: Mice containing the liver-protecting genetically engineered cell implant showed no signs indicative of parenchymal necrosis and inflammatory cell infiltrations that are typically observed following liver injury (Fig. 6; Supplementary Fig. 5).

Discussion

Synthetic biology, the engineering science of reassembling standardized biological parts in a systematic, rational and predictable manner to program novel cellular behaviour, has enabled the design of theranostic circuits that seamlessly couple biosensor-based detection of disease metabolites to an automated and self-sufficient expression of therapeutic transgenes [38,42–44]. By functionally interconnecting the bile acid sensor TGR5 via a synthetic signalling cascade to a modified promoter and expression of the biopharmaceutical HGF, we have designed a theranostic liver-protection device that enables genetically engineered cells to interface with the host metabolism by constantly measuring SBA levels. Whenever SBA levels reach a critical concentration

indicative of liver damage, the liver-protection device coordinated the production of HGF in a closed-loop manner by matching diagnosis of liver injuries with liver-protecting therapy. Importantly, the human TGR5 receptor used as the sensor component for the liver-protection device is sensitive to a variety of endogenous serum bile acids within their clinically relevant concentration range and drives expression of therapeutic HGF levels exclusively at pathologic SBA levels. Since TGR5 is also responsive to the potential antidiabetic drug TUDCA, the bile acid sensor might also be used in future gene therapy applications that couple drug-based diabetes therapy with expression of complementary biopharmaceuticals [45].

Drug-induced hepatotoxicity remains a major challenge in the treatment of various diseases such as multidrug-resistant tuberculosis [46] and colorectal cancer [47]. 20% of the patients diagnosed with colorectal cancer have distant metastases, primarily in the liver. Surgical resection of isolated liver metastases is the treatment of choice [48]. When the metastases are too big for primary surgical resection patients are first treated with chemotherapeutic drugs aiming for size reduction that could render them resectable [49]. However, this approach is limited by the hepatotoxicity of the chemotherapeutic agents such as Irinotecan or Oxaliplatin, which may trigger chemotherapy-associated steatohepatitis, vascular injury and non-cirrhotic portal hypertension [50]. The liver-protection device may protect

Research Article
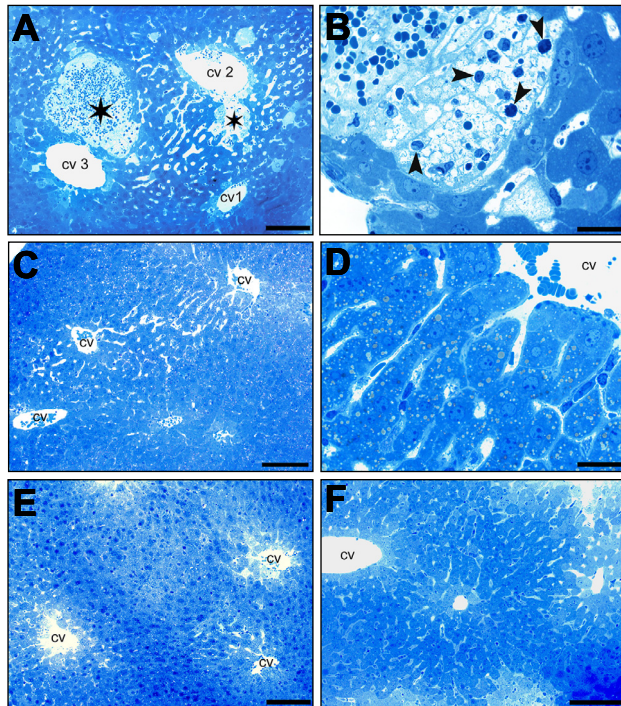
Fig. 6. Toluidine blue-based histological analysis of liver damage in animals treated with the liver-protection device. (A–F) Animals received either no implant or genetically engineered cell implants (5×10^6 cells, 25000 capsules, 200 cells/capsule) containing the liver-protection device (pPB2/pPB5; P_{hCMV^*-1}-TGR5-pA/P_{CREm}-HGF-pA), the placebo device (pPB2/pSP16; P_{hCMV^*-1}-TGR5-pA/P_{CREm}-SEAP-pA; negative control) or a constitutive HGF expression unit (pPB7; P_{hCMV}-HGF-pA; positive control) and were treated with a single dose of either ANIT (75 mg/kg in olive oil) or the diluent olive oil (8 ml/kg). (A, B) ANIT-treated animals exhibiting gradually-cumulative lesions characterized by necrotic and hemorrhagic lesions (asterisk) located close to the central veins (cv). The pathohistological changes revealed as the entire sequence from normal appearance (cv1) to dilated sinusoids (cv2) and necrotic lesions (cv3) containing infiltrations of macrophages and granulocytes (arrowhead). (B, larger magnification of A; Scale bar A = 100 μm, B = 20 μm). (C, D) ANIT-treated mice containing the liver-protection device show slightly dilated sinusoidal vessels without pathological changes (D, larger magnification of C; scale bars 100 μm (C), 20 μm (D)). (E) Control animals treated with placebo implants and olive oil exhibit normal liver structures (scale bar 100 μm). (F) Control animals treated with ANIT and constitutive HGF production implants show normal liver structures (scale bar 100 μm). (This figure appears in colour on the web.)

the liver during the treatment of patients with higher doses of chemotherapeutics.

Drug-induced hepatotoxicity is an important concern in the treatment of tuberculosis, in particular multidrug-resistant tuberculosis, whose prevalence has reached 20% of treated cases [46]. The first-line treatment of this infectious disease includes Isoniazid and Rifampicin, which are hepatotoxic especially when administered at higher doses [51,52]. Indeed, liver failure associated with anti-tuberculosis treatment is the most common acute drug-associated liver failure in South Asia [53]. HGF has been shown to exert liver-protective effects against Isoniazid- and Rifampicin-induced liver damage [54]. The use of a liver-protection device that reversibly triggers the production and secretion of HGF in response to developing liver damage by sensing bile acids may enable the use of anti-tuberculosis drugs at higher doses while limiting the damage to the liver.

The poor pharmacokinetics of HGF so far precludes the use of this potent biopharmaceutical. *In situ* production of HGF using a gene therapy-based approach has in principle confirmed HGF's potential for the treatment of liver injuries and other organ insufficiencies such as diabetic neuropathy, critical limb ischemia and ischemic cardiac disease [18–21,55]. However, the classic gene-based treatment strategy lacks the expression dynamics and interface with the host metabolism that is required to adapt HGF production to the disease course in real time. Additionally, chronic activation of the HGF receptor is associated with a variety of cancer types [56,57], which highlights the importance of a self-sufficient HGF production provided by the closed-loop liver-protection device when targeting potentially fatal hepatotoxic drug effects.

Although the liver-protection device exclusively contains human genetic components, is engineered into human cells, and responds to clinically relevant SBA levels, there are still several translational challenges before genetically engineered theranostic cells will be routinely used for human therapy. To adapt genetically engineered theranostic cells to the clinic, critical design parameters will have to be addressed, including the use of autologous cells, scaling of the system to provide therapeutic levels of HGF, and development of an implant that stores the genetically engineered cells in a single device. The final therapy may be based on patient-derived autologous cell batches that are produced, engineered with the liver-protection device, validated for optimal patient-specific response and dosing performance and frozen for storage. The genetically engineered cells will be filled into appropriate containers and implanted into the body where they automatically connect to the bloodstream [33], monitor SBA levels and corresponding liver damage and coordinate the therapeutic response. The genetically engineered cell implants will be preferably placed subcutaneously, since they can be removed by a minimal ambulant intervention in case of complications or replaced at regular intervals (e.g., every 3–4 months) due to fibrosis.

In summary, protection of the liver from drug-induced toxicities by an engineered theranostic liver-protection device may enable novel and/or more aggressive treatments of diseases where the use of current armamentarium is limited by severe hepatic toxicity.

Financial support

Conflict of interest

The authors who have taken part in this study declared that they do not have anything to disclose regarding funding or conflict of interest with respect to this manuscript.

Authors' contributions

P.B., M.X., H.Y., V.D. and M.F. designed the project, P.B., M.X., H.Y., P.S., H.Z., V.D. and M.F. analysed the results and wrote the manuscript. P.B., V.D. and G.C-E.H. performed the experimental work.

Molecular and Cell Biology

Supplementary data

Supplementary data associated with this article can be found, in the online version, at http://dx.doi.org/10.1016/j.jhep.2016.03.020.

References

Author names in bold designate shared co-first authorship

[1] Bhatia Sangeeta N, Underhill Gregory H, Zaret Kenneth S, Fox Ira J. Cell and tissue engineering for liver disease. Sci Transl Med 2014;6:1–21.

[2] Thomas C, Pellicciari R, Pruzanski M, Auwerx J, Schoonjans K. Targeting bile-acid signalling for metabolic diseases. Nat Rev Drug Discov 2008;7:678–693.

[3] Hofmann AF. Bile acids: trying to understand their chemistry and biology with the hope of helping patients. Hepatology 2009;49:1403–1418.

[4] Glantz A, Marschall HU, Mattsson LA. Intrahepatic cholestasis of pregnancy: Relationships between bile acid levels and fetal complication rates. Hepatology 2004;40:467–474.

[5] Ferraris R, Colombatti G, Fiorentini MT, Carosso R, Arossa W, De La Pierre M. Diagnostic value of serum bile acids and routine liver function tests in hepatobiliary diseases. Dig Dis Sci 1983;28:129–136.

[6] Trinchet J-C, Gerhardt M-F, Balkau B, Munz C, Poupon RE. Serum bile acids and cholestasis in alcoholic hepatitis. Relationship with usual liver tests and histological features. J Hepatol 1994;21:235–240.

[7] Douglas JG, Beckett GJ, Nimmo IA, Finlayson ND, Percy-Robb IW. Clinical value of bile salt tests in anicteric liver disease. Gut 1981;22:141–148.

[8] Shlomai A, Halfon P, Goldiner I, Zelber-Sagi S, Halpern Z, Oren R, et al. Serum bile acid levels as a predictor for the severity of liver fibrosis in patients with chronic hepatitis C. J Viral Hepat 2013;20:95–102.

[9] Barnes S, Gallo GA, Trash DB, Morris JS. Diagnositic value of serum bile acid estimations in liver disease. J Clin Pathol 1975;28:506–509.

[10] Neale G, Lewis B, Weaver V, Panveliwalla D. Serum bile acids in liver disease. Gut 1971;12:145–152.

[11] Fan M, Wang X, Xu G, Yan Q, Huang W. Bile acid signaling and liver regeneration. Biochim Biophys Acta 2015;1849:196–200.

[12] Pean N, Doignon I, Garcin I, Besnard A, Julien B, Liu B, et al. The receptor TGR5 protects the liver from bile acid overload during liver regeneration in mice. Hepatology 2013;58:1451–1460.

[13] Taub R. Liver regeneration: from myth to mechanism. Nat Rev Mol Cell Biol 2004;5:836–847.

[14] Nakamura T, Mizuno S. The discovery of Hepatocyte Growth Factor (HGF) and its significance for cell biology, life sciences and clinical medicine. Proc Jpn Acad Ser B Phys Biol Sci 2010;86:588–610.

[15] Nakamura T, Sakai K, Nakamura T, Matsumoto K. Hepatocyte growth factor twenty years on: Much more than a growth factor. J Gastroenterol Hepatol 2011;26:188–202.

[16] Tsochatzis EA, Bosch J, Burroughs AK. Liver cirrhosis. Lancet 2014;383:1749–1761.

[17] Williams R, Aspinall R, Bellis M, Camps-Walsh G, Cramp M, Dhawan A, et al. Addressing liver disease in the UK: a blueprint for attaining excellence in health care and reducing premature mortality from lifestyle issues of excess consumption of alcohol, obesity, and viral hepatitis. Lancet 2014;384:1953–1997.

[18] Kessler JA, Smith AG, Cha B-S, Choi SH, Wymer J, Shaibani A, et al. Double-blind, placebo-controlled study of HGF gene therapy in diabetic neuropathy. Ann Clin Transl Neurol 2015;2:465–478.

[19] Powell RJ, Simons M, Mendelsohn FO, Daniel G, Henry TD, Koga M, et al. Results of a double-blind, placebo-controlled study to assess the safety of intramuscular injection of hepatocyte growth factor plasmid to improve limb perfusion in patients with critical limb ischemia. Circulation 2008;118:58–65.

[20] Shigematsu H, Yasuda K, Iwai T, Sasajima T, Ishimaru S, Ohashi Y, et al. Randomized, double-blind, placebo-controlled clinical trial of hepatocyte growth factor plasmid for critical limb ischemia. Gene Ther 2010;17:1152–1161.

[21] Yuan B, Zhao Z, Zhang Y-R, Wu C-T, Jin W-G, Zhao S, et al. Short-term safety and curative effect of recombinant adenovirus carrying hepatocyte growth factor gene on ischemic cardiac disease. In Vivo 2008;22:629–632.

[22] **Simonsen JL**, **Rosada C**, Serakinci N, Justesen J, Stenderup K, Rattan SIS, et al. Telomerase expression extends the proliferative life-span and maintains the osteogenic potential of human bone marrow stromal cells. Nat Biotechnol 2002;20:592–596.

[23] Wieland M, Ausländer D, Fussenegger M. Engineering of ribozyme-based riboswitches for mammalian cells. Methods 2012;56:351–357.

[24] Rössger K, Charpin-El Hamri G, Fussenegger M. Reward-based hypertension control by a synthetic brain–dopamine interface. Proc Natl Acad Sci U S A 2013;110:18150–18155.

[25] Tubio MR, Fernandez N, Fitzsimons CP, Copsel S, Santiago S, Shayo C, et al. Expression of a G Protein-coupled Receptor (GPCR) leads to attenuation of signaling by other GPCRs: experimental evidence for a spontaneous GPCR constitutive inactive form. J Biol Chem 2010;285:14990–14998.

[26] Bentayeb K, Batlle R, Sanchez C, Nerin C, Domeno C. Determination of bile acids in human serum by on-line restricted access material-ultra high-performance liquid chromatography-mass spectrometry. J Chromatogr B Analyt Technol Biomed Life Sci 2008;869:1–8.

[27] Solá S, Garshelis DL, Amaral JD, Noyce KV, Coy PL, Steer CJ, et al. Plasma levels of ursodeoxycholic acid in black bears, Ursus americanus: Seasonal changes. Comp Biochem Physiol C Toxicol Pharmacol 2006;143:204–208.

[28] Alnouti Y, Csanaky IL, Klaassen CD. Quantitative-profiling of bile acids and their conjugates in mouse liver, bile, plasma, and urine using LC-MS/MS. J Chromatogr B Analyt Technol Biomed Life Sci 2008;873:209–217.

[29] Ozcan U, Yilmaz E, Ozcan L, Furuhashi M, Vaillancourt E, Smith RO, et al. Chemical chaperones reduce ER stress and restore glucose homeostasis in a mouse model of type 2 diabetes. Science 2006;313:1137–1140.

[30] Kars M, Yang L, Gregor MF, Mohammed BS, Pietka TA, Finck BN, et al. Tauroursodeoxycholic Acid may improve liver and muscle but not adipose tissue insulin sensitivity in obese men and women. Diabetes 2010;59:1899–1905.

[31] Ye H, Daoud-El Baba M, Peng RW, Fussenegger M. A synthetic optogenetic transcription device enhances blood-glucose homeostasis in mice. Science 2011;332:1565–1568.

[32] Cervera L, Gutierrez S, Godia F, Segura M. Optimization of HEK 293 cell growth by addition of non-animal derived components using design of experiments. BMC Proc 2011;5:P126.

[33] Jacobs-Tulleneers-Thevissen D, Chintinne M, Ling Z, Gillard P, Schoonjans L, Delvaux G, et al. Sustained function of alginate-encapsulated human islet cell implants in the peritoneal cavity of mice leading to a pilot study in a type 1 diabetic patient. Diabetologia 2013;56:1605–1614.

[34] Xue F, Takahara T, Yata Y, Minemura M, Morioka CY, Takahara S, et al. Attenuated acute liver injury in mice by naked hepatocyte growth factor gene transfer into skeletal muscle with electroporation. Gut 2002;50:558–562.

[35] Harris EH. Elevated Liver Function Tests in Type 2 Diabetes. Clin Diabetes 2005;23:115–119.

[36] Manibur Rahman Tony, Hodgson Humphrey JF. Animal models of acute hepatic *failure*. Int J Exp Pathol 2000;81:145–157.

[37] Liu Y, Binz J, Numerick MJ, Dennis S, Luo G, Desai B, et al. Hepatoprotection by the farnesoid X receptor agonist GW4064 in rat models of intra- and extrahepatic cholestasis. J Clin Invest 2003;112:1678–1687.

[38] Heng BC, Aubel D, Fussenegger M. Prosthetic gene networks as an alternative to standard pharmacotherapies for metabolic disorders. Curr Opin Biotechnol 2015;35C:37–45.

[39] Kosai K, Matsumoto K, Funakoshi H, Nakamura T. Hepatocyte growth factor prevents endotoxin-induced lethal hepatic failure in mice. Hepatology 1999;30:151–159.

[40] Xue F, Takahara T, Yata Y, Kuwabara Y, Shinno E, Nonome K, et al. Hepatocyte growth factor gene therapy accelerates regeneration in cirrhotic mouse livers after hepatectomy. Gut 2003;52:694–700.

[41] Kawaida K, Matsumoto K, Shimazu H, Nakamura T. Hepatocyte growth factor prevents acute renal failure and accelerates renal regeneration in mice. Proc Natl Acad Sci U S A 1994;91:4357–4361.

Molecular and Cell Biology

Research Article

[42] Kemmer C, Gitzinger M, Daoud-El Baba M, Djonov V, Stelling J, Fussenegger M. Self-sufficient control of urate homeostasis in mice by a synthetic circuit. Nat Biotechnol 2010;28:355–360.

[43] Rossger K, Charpin-El-Hamri G, Fussenegger M. A closed-loop synthetic gene circuit for the treatment of diet-induced obesity in mice. Nat Commun 2013;4:2825.

[44] Auslander D, Auslander S, Charpin-El Hamri G, Sedlmayer F, Muller M, Frey O, et al. A synthetic multifunctional mammalian pH sensor and CO_2 transgene-control device. Mol Cell 2014;55:397–408.

[45] Ye H, Charpin-El Hamri G, Zwicky K, Christen M, Folcher M, Fussenegger M. Pharmaceutically controlled designer circuit for the treatment of the metabolic syndrome. Proc Natl Acad Sci U S A 2013;110:141–146.

[46] WHO. Global tuberculosis report 2012. Geneva, Switzerland: World Health Organization Press; 2012.

[47] Siegel R, DeSantis C, Jemal A. Colorectal cancer statistics, 2014. CA Cancer J Clin 2014;64:104–117.

[48] Kopetz S, Chang GJ, Overman MJ, Eng C, Sargent DJ, Larson DW, et al. Improved survival in metastatic colorectal cancer is associated with adoption of hepatic resection and improved chemotherapy. J Clin Oncol 2009;27:3677–3683.

[49] Reddy SK, Zorzi D, Lum YW, Barbas AS, Pawlik TM, Ribero D, et al. Timing of multimodality therapy for resectable synchronous colorectal liver metastases: a retrospective multi-institutional analysis. Ann Surg Oncol 2009;16:1809–1819.

[50] Cleary JM, Tanabe KT, Lauwers GY, Zhu AX. Hepatic toxicities associated with the use of preoperative systemic therapy in patients with metastatic colorectal adenocarcinoma to the liver. Oncologist 2009;14:1095–1105.

[51] Graham SM. Treatment of paediatric TB: revised WHO guidelines. Paediatr Respir Rev 2011;12:22–26.

[52] Weber W, Schoenmakers R, Keller B, Gitzinger M, Grau T, Daoud-El Baba M, et al. A synthetic mammalian gene circuit reveals antituberculosis compounds. Proc Natl Acad Sci U S A 2008;105:9994–9998.

[53] Kumar R, Shalimar Bhatia V, Khanal S, Sreenivas V, Gupta SD, et al. Antituberculosis therapy–induced acute liver failure: magnitude, profile, prognosis, and predictors of outcome. Hepatology 2010;51:1665–1674.

[54] Enriquez-Cortina C, Almonte-Becerril M, Clavijo-Cornejo D, Palestino-Domínguez M, Bello-Monroy O, Nuño N, et al. Hepatocyte growth factor protects against isoniazid/rifampicin-induced oxidative liver damage. Toxicol Sci 2013;135:26–36.

[55] Matsuno Y, Iwata H, Umeda Y, Takagi H, Mori Y, Kosugi A, et al. Hepatocyte growth factor gene transfer into the liver via the portal vein using electroporation attenuates rat liver cirrhosis. Gene Ther 2003;10:1559–1566.

[56] Christensen JG, Burrows J, Salgia R. C-Met as a target for human cancer and characterization of inhibitors for therapeutic intervention. Cancer Lett 2005;225:1–26.

[57] Maroun CR, Rowlands T. The Met receptor tyrosine kinase: a key player in oncogenesis and drug resistance. Pharmacol Ther 2014;142:316–338.

[58] Morgenstern JP, Land H. Advanced mammalian gene transfer: high titre retroviral vectors with multiple drug selection markers and a complementary helper-free packaging cell line. Nucleic Acids Res 1990;18:3587–3596.

[59] Gupta PB, Kuperwasser C, Brunet J-P, Ramaswamy S, Kuo W-L, Gray JW, et al. The melanocyte differentiation program predisposes to metastasis following neoplastic transformation. Nat Genet 2005;37:1047–1054.

[60] Kemmer C, Fluri DA, Witschi U, Passeraub A, Gutzwiller A, Fussenegger M. A designer network coordinating bovine artificial insemination by ovulation-triggered release of implanted sperms. J Control Release 2011;150:23–29.

[61] Fussenegger M, Mazur X, Bailey JE. A novel cytostatic process enhances the productivity of Chinese hamster ovary cells. Biotechnol Bioeng 1997;55:927–939.

[62] Keeley M, Busch J, Singh R, Abel T. TetR hybrid transcription factors report cell signaling and are inhibited by doxycycline. Biotechniques 2005;39:529–536.

[63] Saxena P, Charpin-El Hamri G, Folcher M, Zulewski H, Fussenegger M. Synthetic gene network restoring endogenous pituitary–thyroid feedback control in experimental Graves' disease. Proc Natl Acad Sci U S A 2016;113:1244–1249.